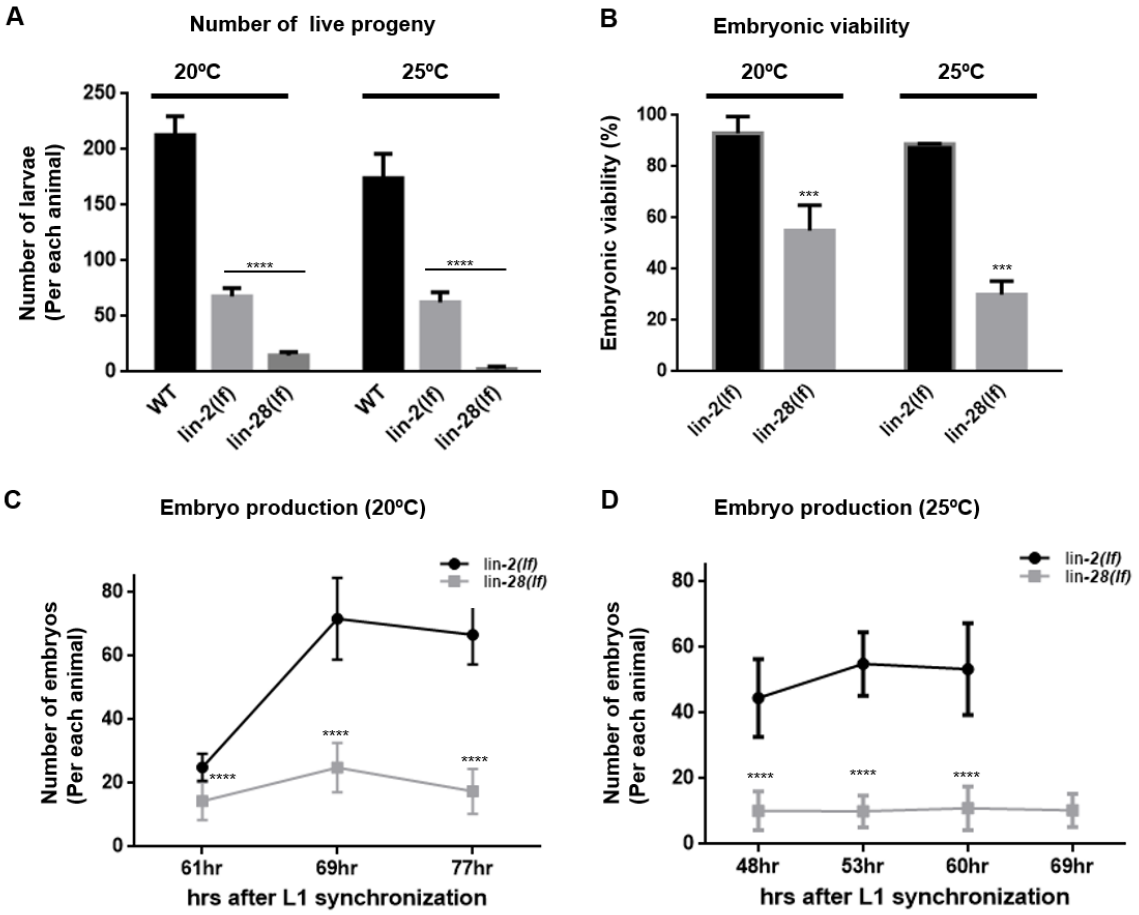

Figure S1. Fertility phenotypes and embryonic viability of *lin-28(lf)* mutants at 20°C and 25°C.

(A)Total number of live larval progeny per animal for wild-type N2 animals(n=5), *lin-2(e1309)* mutants(n=17 for 25°C, n=16 for 20°C) and *lin-28(n719)* (n=19) mutants at 20°C and 25°C. (B) Embryonic viability for *lin-2(e1309)* and *lin-28(n719)* mutants at 20°C and 25°C. (Number of animlals≥15 per each assay; number of independent replicate assays = 3) (C) The number of embryos produced at varying time points after feeding of synchronized L1 larvae, for *lin-2(e1309)* and *lin-28(n719)* mutants at 20°C and 25°C. (n= 10,8,8 (*lin-2(e1039*), 12,15,13 (*lin-28(n719)*) for 61hr, 69hr, and 77hr respectively at 20°C. n= 12,10,10, 0(*lin-2(e1039*), 15,13,12,3 (*lin-28(n719)*) for 48hr, 53hr, 60hr and 69hr respectively at 25°C.) (A-C: Data are shown as mean ± SD. Unpaired t-test compared to *lin-2(lf)*, ****p<0.0001)

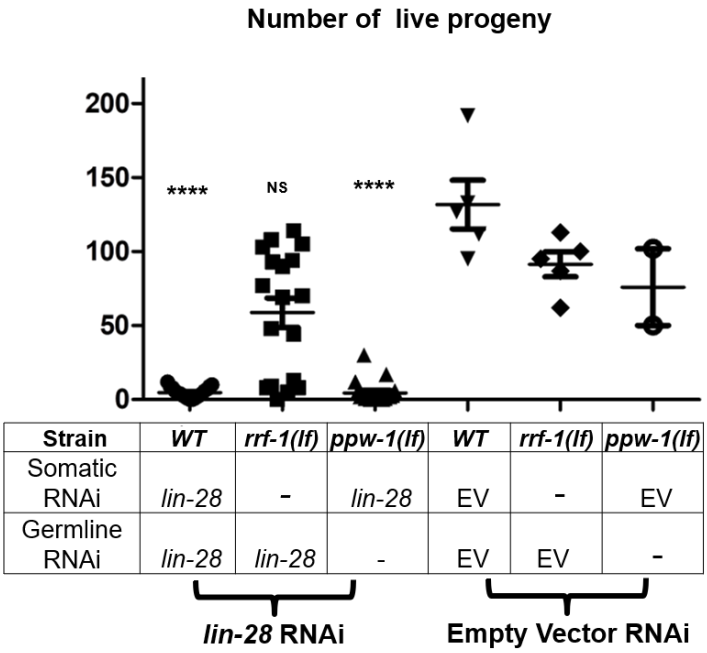

Figure S2. Reduction of *lin-28* function in the soma decreases fertility of hermaphrodites more than does reduction of *lin-28* function in the germline.

Wild type, *rrf-1(pk1417)* mutants, and *ppw-1(pk2505)* mutants were fed with *lin-28* RNAi and empty vector RNAi, and the number of progeny produced by each animal was determined. *ppw-1(pk2505) lin-28(RNAi)* animals all exhibited reduced fertility similar to *lin-28(RNAi)* animals. However, *rrf-1(pk1417) lin-28(RNAi)* animals were, overall, less affected by *lin-28(RNAi)*, with only a minority of animals exhibiting reduced fertility. (Error bar shows standard deviation. unpaired t-test, each strain with *lin-28*(RNAi) was compared to corresponding strain with empty vector(RNAi). NS; not significant, ****p<0.0001.)

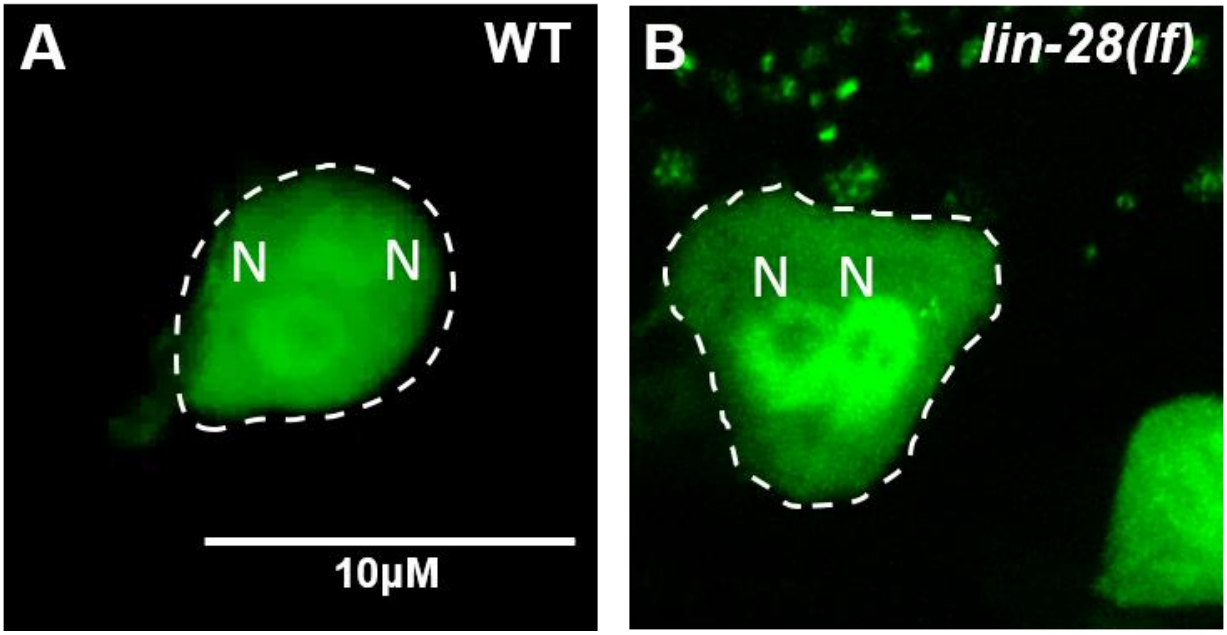

Figure S3. Both wild type and *lin-28(lf)* mutants have two nuclei that comprise Sp-Ut valve core syncytium.

Confocal microscopic images of Sp-Ut valve core syncytium labeled by *cog-1::GFP*. Both wild type animals (A) and *lin-28(lf)* mutants (B) exhibit two nuclei in their Sp-Ut valve core region (outlined), suggesting cell division in the Sp-Ut valve core occurs normally in *lin-28(lf)* mutants. Scale bar = 10 μm.

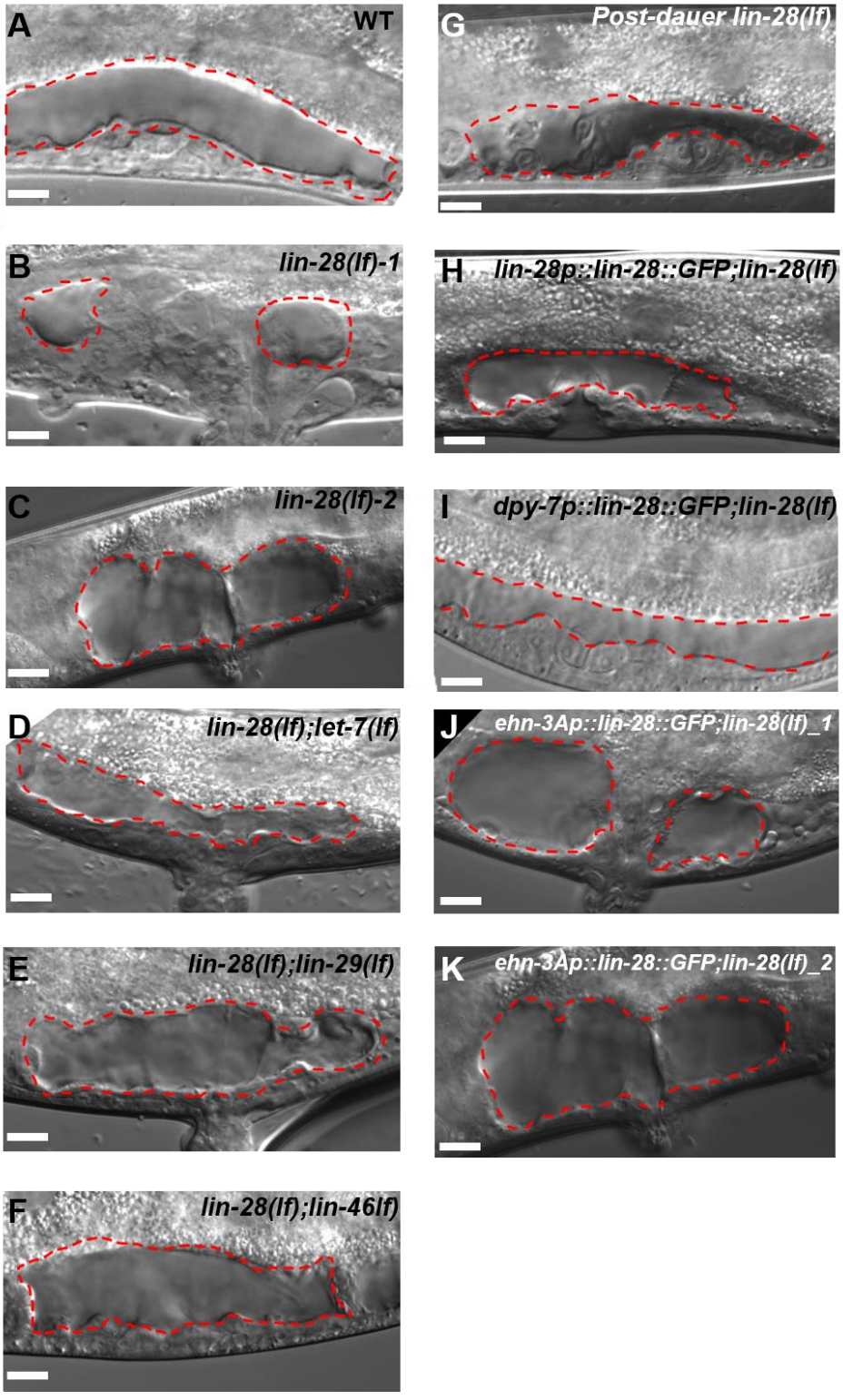

Figure S4. Defective formation of the uterine lumen in *lin-28(lf)* mutants is restored by the loss of function of *lin-28* downstream genes, post-dauer development, or hypodermal *lin-28* expression. (A-C) Uterine lumen formation in wild type and *lin-28(n719)* mutants. (A) Wild-type animals form a long uterine lumen between the dorsal uterus and ventral uterus in the mid L4 stage (outlined), whereas, (B) the majority of *lin-28(n719)* mutants at an analogous point in 4th stage development exhibit an immature, partially-formed lumen. (C) Some 4th stage *lin-28(n719)* mutants show a connected lumen, which is shorter and rounder than that in wild-type animals. (D-F) Uterine lumen formation in *lin-28(n719);let-7(mn112), lin-28(n719);lin-29(n836)*,and *lin-28(n719);lin-46(ma164)* double mutants. (D) Uterine lumen formation is restored in ~50% of *lin-28(n719);let-7(mn112)* mutants. (E) The majority of *lin-28(n719);lin-29(n836)* animals, and (F) the majority of *lin-28(n719);lin-46(ma164)* mutants show uterine lumen formation similar to the wild type. (G) *lin-28(n719)* mutants form an elongated uterine lumen similar to wild type after post-dauer development. (H-K) Rescue of *lin-28(lf)* uterine lumen phenotype by transgenes expressing LIN-28 driven by specific promotors. *lin-28p::lin-28::GFP;lin-28(n719)* (H) and *dpy-7p::lin-28::GFP;lin-28(n719)* (I) show normal uterine lumen formation as wild-type animals. *ehn-3Ap::lin-28::GFP;lin-28(n719)* show only partial uterine lumen (J) or shorter and rounder uterine lumen (K) similar to the defects exhibited by *lin-28(n719)* alone (B and C, respectively). Scale bar = 10 µm.

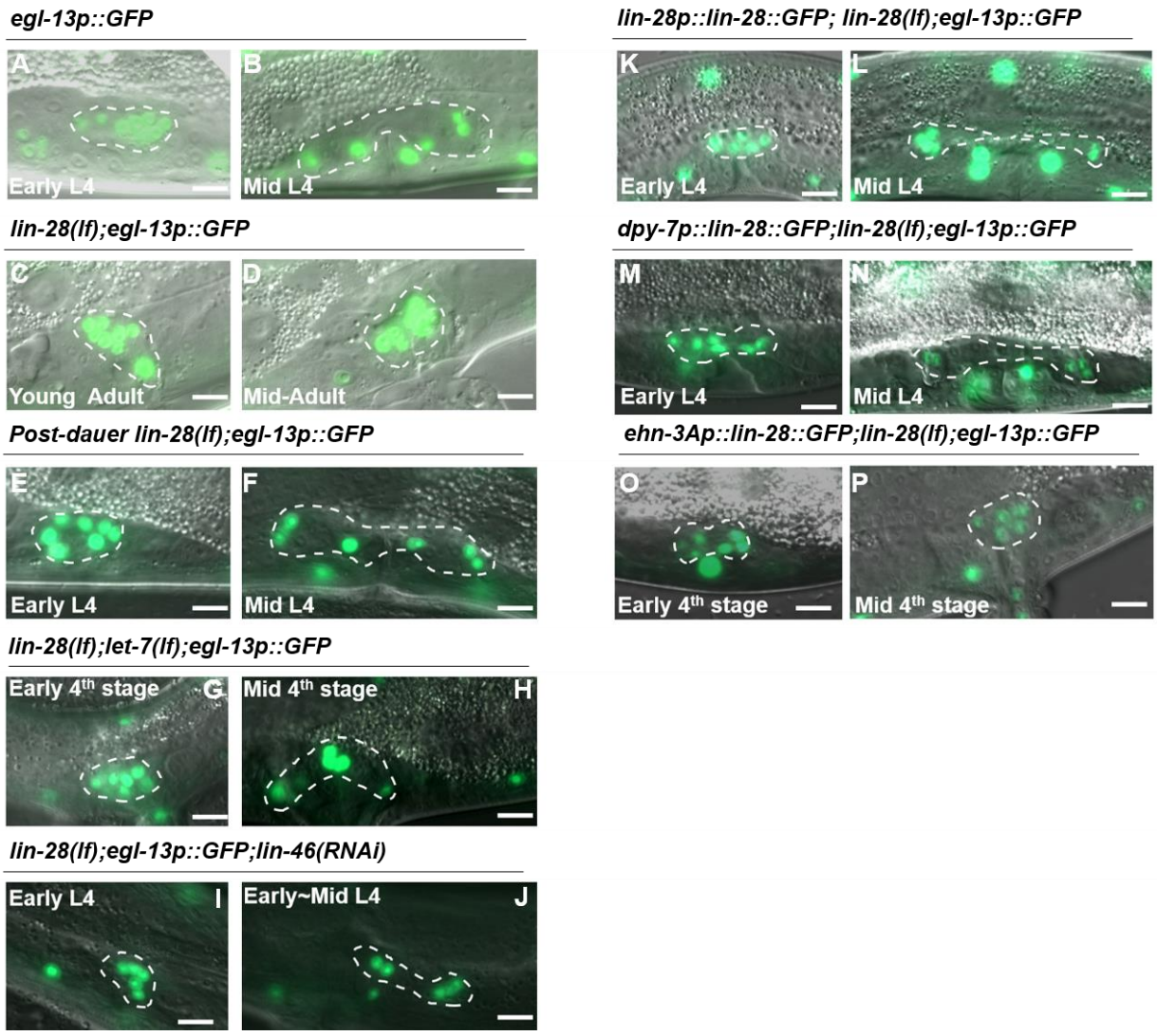

Figure S5. Defective migration of uterine seam (utse) cell nuclei in *lin-28(lf)* mutants is rescued by loss of function of *lin-28* downstream genes, by post-dauer development, or by hypodermal *lin-28* expression. (A-D) utse cell nuclei, labeled by *egl-13p::GFP*, in wild type and *lin-28(n719)* mutants. *egl-13p::GFP* expression in the utse region (outlined) is shown in early L4 (A) and mid-L4 (B) of the wild-type, and at analogous stage (C, D) of 4th stage *lin-28(n719)* animals. utse nuclei expressing *egl-13p::GFP* migrate laterally during the early to mid L4 stage in wild type (A. B), but no such migration occurs in *lin-28(n719)* mutants (C, D). (E,F) utse migration defects of *lin-28(n719)* mutants are suppressed when the mutants develop via post-dauer stages. (G-J) Loss of function of *let-7* or *lin-46* can partially suppress the utse migration defects in *lin-28(lf)* mutants. (G,H) *lin-28(n719);let-7(mn112)* mutants show a more normal migration of utse nuclei compared to *lin-28(n719)* mutants (C, D). (I,J) utse nuclei of *lin-28(n719)* mutants migrated laterally when *lin-46* function was knocked down by RNAi. (K-P) Rescue of *lin-28(lf)* utse migration phenotype by transgenes expressing LIN-28 driven by specific promotors. *lin-28* expression with *lin-28* endogenous promoter (*lin-28p::lin-28::GFP;lin-28(n719);egl-13p::GFP*) restores utse migration as wild type (K, L). Hypodermal expression of *lin-28* (*dpy-7p::lin-28::GFP;lin-28(n719);egl-13p::GFP*) also rescues utse migration defects in *lin-28(n719)* mutants (M, N), whereas *lin-28* expression driven by early somatic gonadal promoter (*ehn-3Ap::lin-28::GFP;lin-28(n719);egl-13p::GFP*) does not rescue the phenotype (O, P). (Note: In these experiments (K-P), the promoter-driven *lin-28* transgene is also tagged with GFP, but *lin-28::GFP* expression is not detectable at these stages, so all the GFP signal here corresponds to *egl-13p::GFP.*).Scale bar = 10 µm.

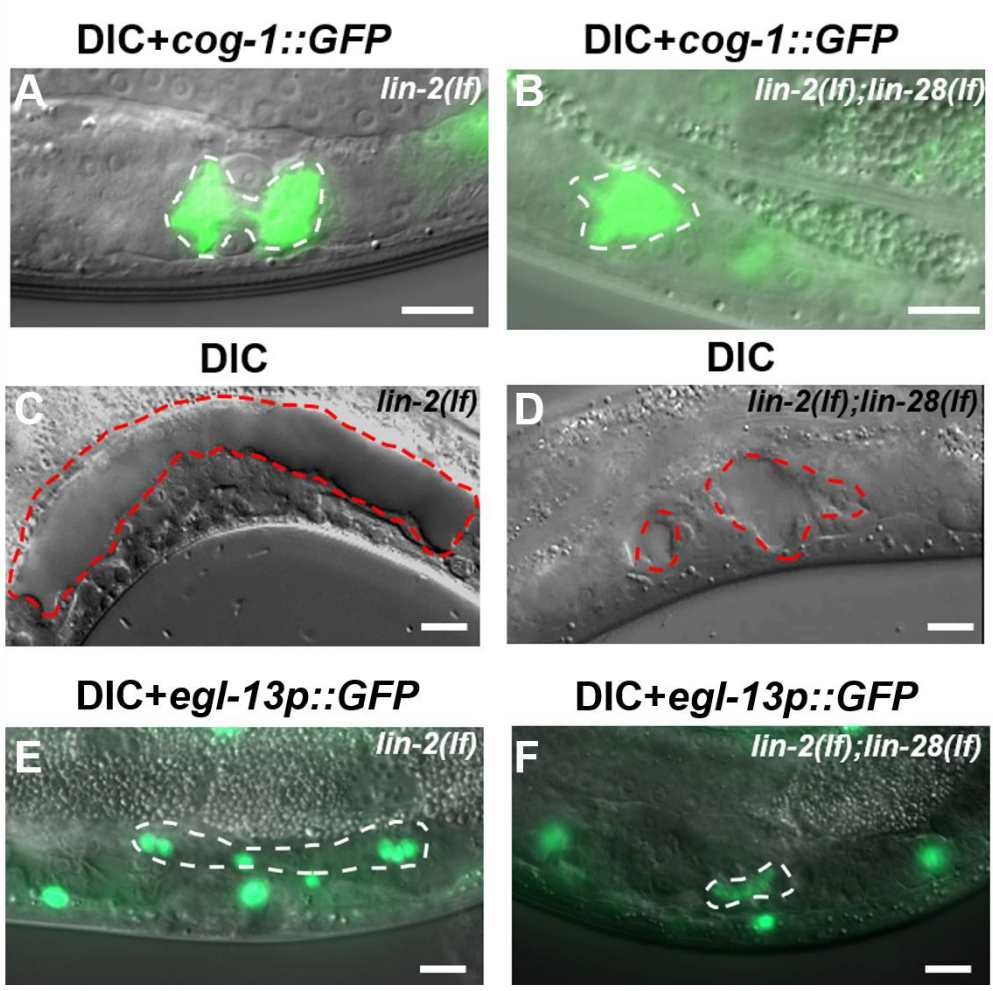

Figure S6. Defective Sp-Ut valve morphogenesis, uterine lumen formation, and utse migration are not results of the abnormal vulval morphogenesis of *lin-28(lf)* animals.

(A, B) Sp-Ut valve core structure (outlined) visualized by *cog-1::GFP* in *lin-2(e1309)* and *lin-2(e1309);lin-28(n719)* animals. (A) The “dumbbell” structure of Sp-Ut valve core cell is shown in *lin-2(e1309)* mutants like wild-type animals (Fig 3C). (B) *lin-2(e1309); lin-28(n719)* mutants exhibit the “single-lobe” structure of Sp-Ut valve core, similar to *lin-28(n719)* mutants (Fig 3D). (C, D) Uterine lumen formation (outlined) visualized by DIC in *lin-2(e1309)* and *lin-2(e1309);lin-28(n719)* animals. (C) Fully extended and connected uterine lumen (outlined) is formed in *lin-2(e1309)* mutants like wild type animals (Fig S4A). (D) By contrast, *lin-2(e1309);lin-28(n719)* mutants form only partial uterine lumen, similar to *lin-28(n719)* (Fig S4B). (E, F) utse nuclei (outlined) are labeled by *egl-13p::GFP* in *lin-2(e1309)* and *lin-2(e1309);lin-28(n719)* animals. (E) utse migration appears normal in *lin-2(e1309)* (Fig S5B), whereas (F) utse nuclei remain tightly clustered in *lin-2(e1309);lin-28(n719)* animals, similar to *lin-28(n719)* (Fig S5D). Scale bar = 10 μm.

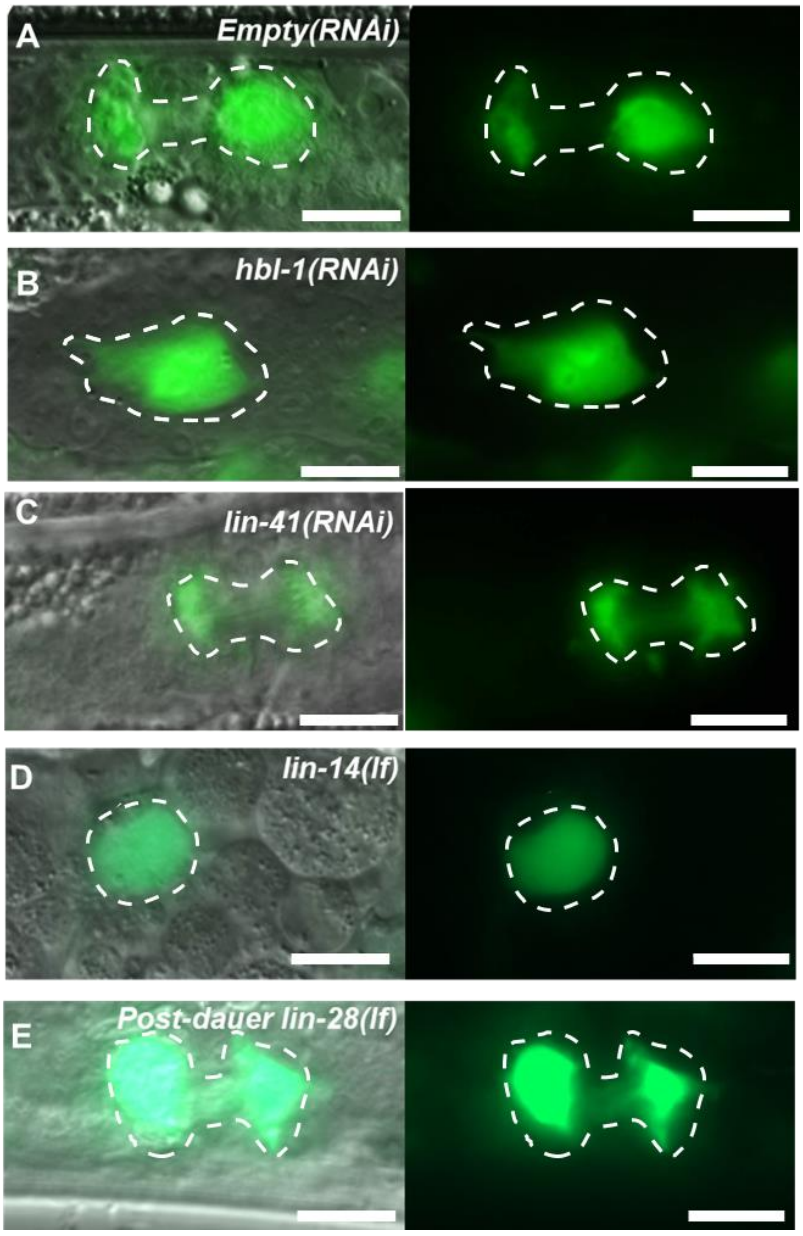

Figure S7. Sp-Ut valve core cell morphology in *hbl-1(lf), lin-41(lf) and lin-14(lf)* mutants, and post-dauer suppression of *lin-28(lf)* morphological defects.

(A-E) Sp-Ut valve core morphology is visualized by *cog-1::GFP,* shown alone (right panel), and overlaid with DIC (left panel). (A) Animals treated with empty vector RNAi have normal Sp-Ut valve morphology. (B) *hbl-1*(RNAi) animals. (C) The Sp-Ut valve of *lin-41*(RNAi) animals appeared essentially normal in morphology, except for a somewhat reduced size. (D) *lin-14(n179)* exhibit abnormal Sp-Ut vavle morphology. (E) Post-dauer development of *lin-28(n719)* mutants restored an Sp-Ut valve morphology similar to wild type animals. Scale bar = 10 µm.

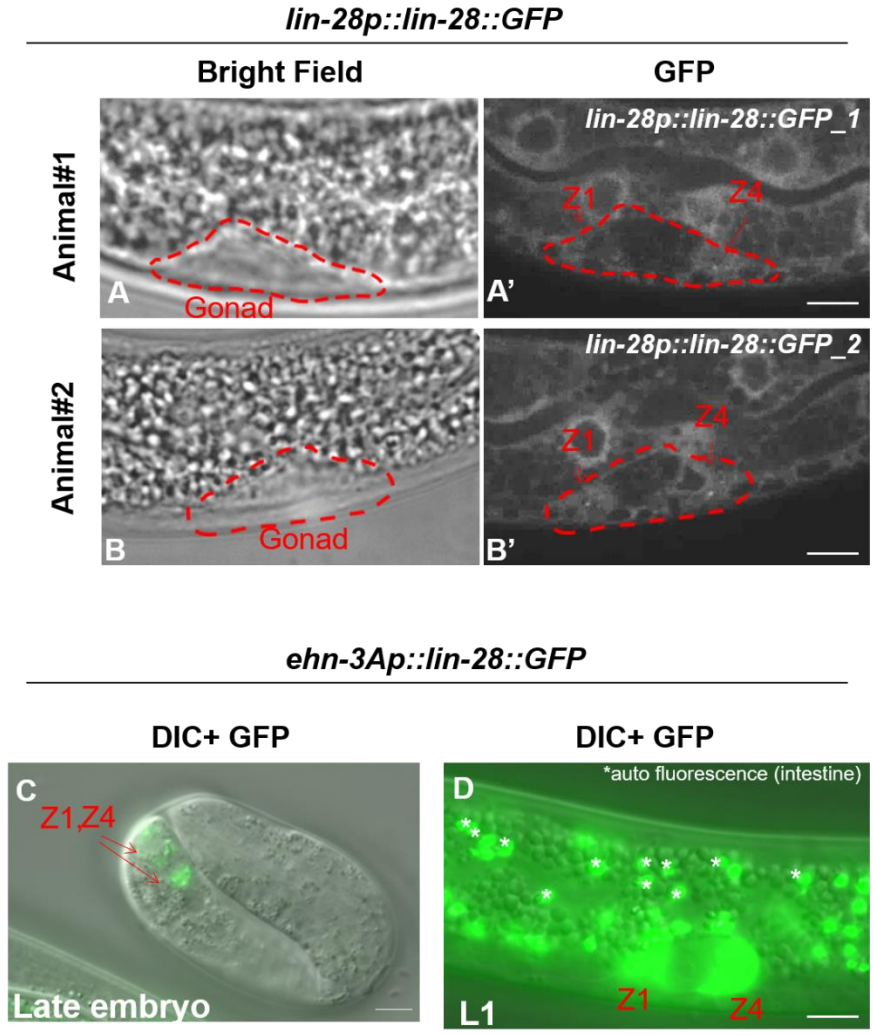

Figure S8. Both *lin-28* endogenous promoter and *ehn-3A* promoter drives early somatic gonadal expression of *lin-28*::GFP.

(A,B) Two *lin-28p::lin-28::GFP* L1 larvae where *GFP* expression was detected in Z1 and Z4 cell by spinning disk microscopy. (C,D) Z1 and Z4 expression of *lin-28::GFP* driven by early somatic gonadal promoter (*ehn-3Ap::lin-28::GFP*). GFP expression in Z1 and Z4 cells were detected by fluorescence microscopy beginning in late embryogenesis (C) also L1 larvae (D). Scale bar = 10 µm.

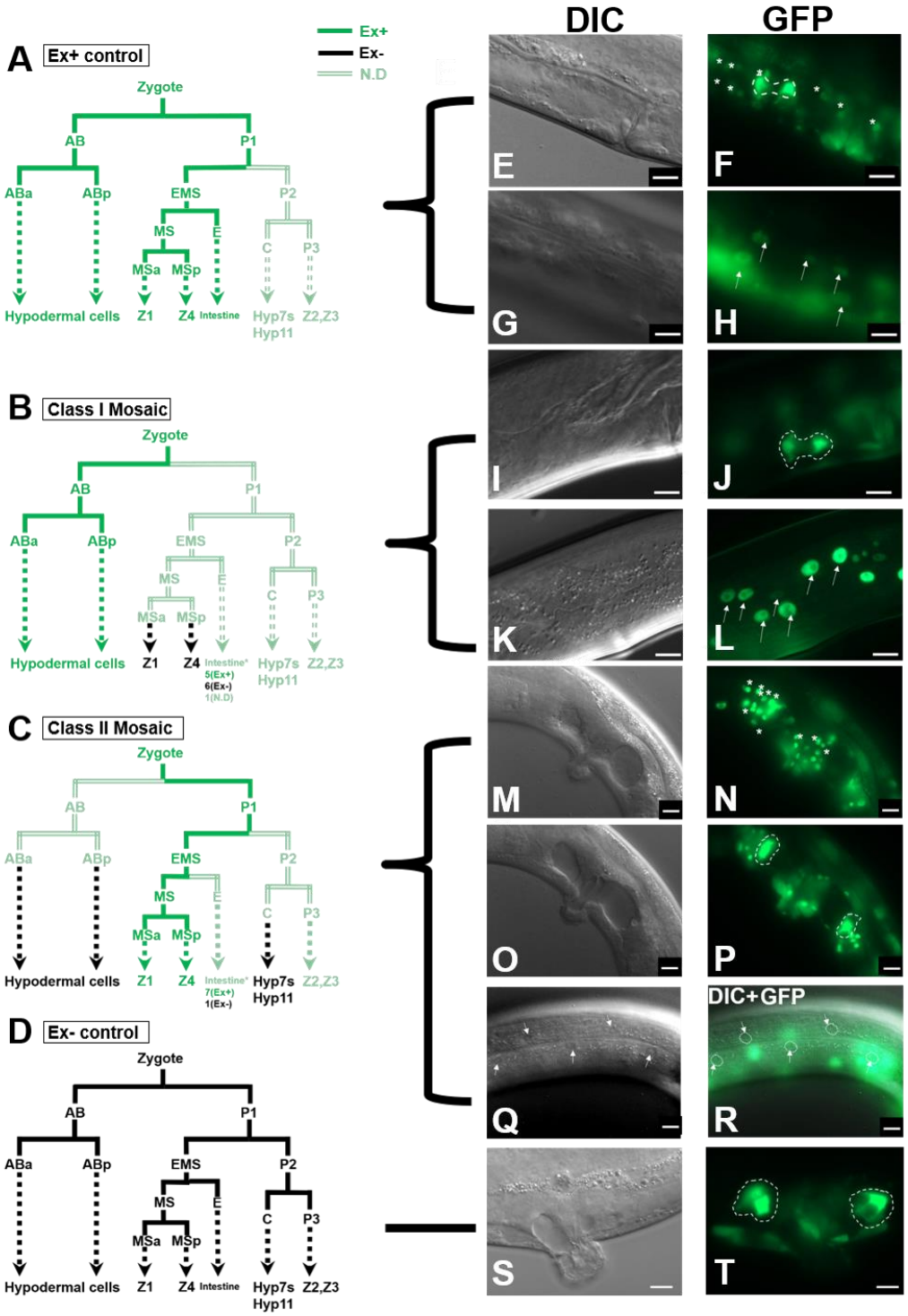

Figure S9. *lin-28(lf)* mosaic analysis for Sp-Ut valve morphogenesis

(A-D) Expression patterns of *sur-5::GFP* in VT3884 animals where the extrachromosomal array maEx265[*sur-5::GFP*; *lin-28p::lin-28::GFP*] was (A) retained in all hypodermal lineages, somatic gonad (Z1,Z4), and intestinal lineages, (B) lost in a precursor to Z1 and Z4, (C) lost in the hypodermal cell lineages, or (D) lost in all cell lineages. The observed *sur-5::GFP* expression patterns are color coded as in Figure 8: Green, confirmed *sur-5::GFP* expression; Black, Confirmed absence of *sur-5::GFP* expression; Light green, *sur-5::GFP* expression not determined. Dotted lines represent multiple cell divisions not shown in these abbreviated cell lineage diagrams. (E-T) Representative DIC or GFP images of animals in each of the indicated classes of animals (A-D). Note that *sur-5::GFP* is expressed only in nucleus and is hence distinctive from *cog-1::GFP* which is expressed also in the cytoplasm. (A, E-H) This category of animals expressed *sur-5::GFP* in (E, F) spermathecal and uterine cells (*), and also in (G, H) hypodermal cells (arrows). Of 44 animals which belong to this category, 43 animals showed dumbbell-shaped Sp-Ut valve core as wild type (F, outlined). (B, I-L) These mosaic animals expressed *sur-5::GFP* in (K, L) hypodermal cell lineages (arrows), but not in (I, J) somatic gonadal lineages. We found 12 mosaic animals showing this pattern and all showed wild type dumbbell-shaped Sp-Ut valve core seen by *cog-1::GFP* (J, outline). 5 animals did and 6 animals did not retain the array in intestinal cell lines. We didn't determine intestinal expression of the array in 1 animal. (C, M-R) In these mosaic animals *sur-5::GFP* was expressed in (M, N) the Z1 and Z4 lineages, but was not detected in (Q, R) the hypodermal lineages. (Q) DIC image of the animal in (R); arrows indicate hypodermal cell nuclei. (R) Merged image of DIC and GFP of the same animal. GFP signals do not match with nucleus of hypodermal cells (outlines) suggesting that GFP signals were not from hypodermal cells. We found 8 mosaic animals in this category, and 7 animals did not have wild type dumbbell-shaped Sp-Ut valve core (P, outline). (Of those 7 animals, 6 animals expressed *sur-5::GFP* in the intestinal (E) cell lineage, and 1 did not express *sur-5::GFP* in the intestine.) 1 animal showed wild type dumbbell-shaped Sp-Ut valve core in anterior somatic gonadal region, but not in posterior region. This animal expressed *sur-5::GFP* in the intestinal region. (D, S, T) Animals that did not express *sur-5::GFP* in any cells: 28 out of 30 such animals showed the single-lobe shaped abnormal Sp-Ut valve core morphology characteristic of *lin-28(lf)* mutants(S,T). Scale bar = 10 µm.

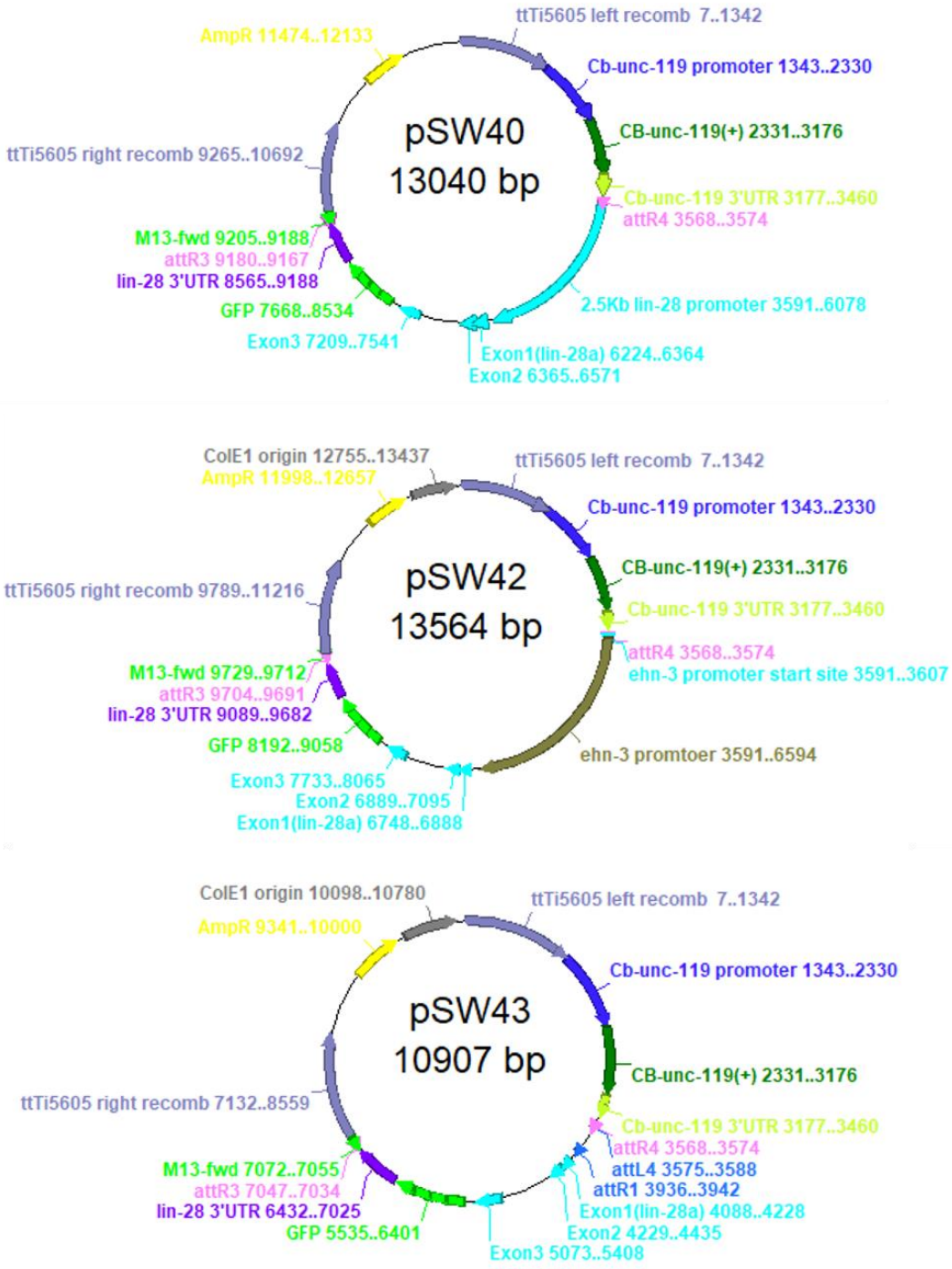

Figure S10. Vector maps of pSW40, pSW42, and pSW43 injected to make transgenic animals.

Table S1. *C. elegans* strains used in this study

Strain Name	Genotype
N2	
VT2932	*lin-28(n719)I*
CB1309	*lin-2(e1309)X*
PS3662	*syIs63[cog-1::GFP + unc-119(+)]*
DZ325	*ezIs2[fkh-6p::GFP + unc-119(+)]; III; him-8(e1489) IV*
VT2929	*lin-28(n719)I;syIs63*
VT2930	*lin-28(n719)I;ezIs2*
VT866	*lin-28(n719)I;let-7(mn112) unc-3(e151) X*
MT2001	*lin-28(n719)I;lin-29(n333) II.*
VT937	*lin-28(n719)I;lin-46(ma164) V*
AG212	*unc-119(ed3); avIs143 [pDNL10 (unc-119(+) + cbd-1p::CBD-1::mCherry::cbd-1 3'UTR)]*
VT3454	*lin-28(n719);avIs143*
UN0810	*fln-1 (tm545)*
VT3660	*lin-14(n179);syIs63*
VT3730	*let-7(mn112);mnDP1;syIs63*
VT3580	*lin-29(n836);syIs63*
VT3581	*lin-46(ma164) maIs105 [col-19::GFP]; syIs63*
MH1319	*kuIs29 [egl-13p::GFP+unc-119(+)]*
VT3661	*lin-28(n719);kuIs29*
VT3731	*lin-28(n719);let-7(mn112);kuIs29*
VT3665	*lin-2(e1309);syIs63*
VT3664	*lin-2(e1309);lin-28(n719);syIs63*
VT3733	*lin-2(e1309);kuIs29*
VT3732	*lin-2(e1309);lin-28(n719);kuIs29*
EG4322	*ttTi5605 II; unc-119(ed3) III;*
WM186	*avr-14(ad1302) I; ttTi5605 II; unc-119(ed3) III; avr-15(ad1051) glc-1(pk54) V*
VT3392	*avr-14(ad1302) I;maIs402[unc-119(+);ehn-3Ap::ln-28:GFP::lin-28 3'UTR];unc-119(ed3) III;avr-15(ad1051) glc-1(pk54) V*
VT3486	*avr-14(ad1302) I;maIs403[unc-119(+);lin-28p::ln-28:GFP::lin-28 3'UTR];unc-119(ed3) III;avr-15(ad1051) glc-1(pk54) V*
VT3702	*maIs409[unc-119(+); dpy-7p::lln-28:GFP::lin-28 3'UTR]II;unc-119(ed3) III*
VT3517	*lin-28(n719);maIs402;syIs63*
VT3516	*lin-28(n719);maIs403;syIs63*
VT3703	*lin-28(n719);maIs409;syIs63*
VT3734	*lin-28(n719);maIs402;kuIs29*
VT3735	*lin-28(n719);maIs403;kuIs29*
VT3736	*lin-28(n719);maIs409;kuIs29*
NL2098	*rrf-1(pk1417)*
NL2550	*ppw-1(pk2505)*
VT3884	*lin-28(n719)I;syIs63;maEx265[sur-5::GFP;lin-28p::GFP;lin-28 3'UTR]*

Table S2. Primer sequences used in this study

	Primers	Sequences	
1	lin-28(n719) genotyping F	ttataaataaaagtcggag	sequencing to confirm n719
2	lin-28(n719) genotyping R	cctttcagtccttgtccttctac	
3	let-7(mn112) genotyping F	gataccatggaggacgacgg	WT :476 bp mn112: 263 bp
4	let-7(mn112) genotyping R	gtagaaaattgcatagttca	
5	lin-29(n836) genotyping F	ggcttatcagtttgatggca	WT:273bp n836: 200bp
6	lin-29(n836) genotyping R	cccgcaaatttccggaatc	
7	lin-46(ma164) genotyping F	gaacttcaagattcctactgtag	sequencing to confirm ma164
8	lin-46(ma164) genotyping R	gaaatcacgacaattgtagacattg	
9	lin-14(n179) genotyping F	gaaacagctccaccactc	sequencing to confirm n179
10	lin-14(n179) genotyping R	gttctgacactggtcgg	
11	attB4+ lin-28 promoter F	ggggcaactttgtatagaaaagttgga tttcggtaaaactcttcaagc	lin-28 Promoter:PCR ampliifed, followed by BP reaction with pDONR P4P1r
12	attB1r+ lin-28 pormoter R	ggggctgctttttgtacaaacttgt cctgaaaaagatttttaaaattttt	
13	attB4+ dpy-7 promoter F	ggggcaactttgtatagaaaagttgga aatctcattccacgatttct	dpy-7 promoter: PCR ampliifed, followed by BP reaction with pDONR P4P1r
14	attB1r + dpy-7 promoter R	ggggctgctttttgtacaaacttgt ttatctggaacaaaatgta	
15	attB4+ehn-3 promoter F	ggggcaactttgtatagaaaagttgga ctaatctagaaaaatacgaca	enh-3A promoter:PCR ampliifed, follwed by BP reaction with pDONR P4P1r
16	attB1r+ ehn-3 promoter R	ggggctgctttttgtacaaacttgt tttgtaatttggaagctgg	
17	attB1+lin-28 gene F	ggggacaagtttgtacaaaaagcaggcttc gttcagcaatgcttttaatta	100bp+lin-28:GFP (P:Primer, T:template, PCR product:A~D) 1. **A**: (P) 20/18, (T) gDNA 2. B: (P) 19/22, (T) gDNA 3. C: (P)20/22 (T) A,B -> Removal of the first exon 4. D: (P) 21/23, (T) XW12 (Wei et al., 2012) 5. E : (P) 17/24 (T) C,D ->GFP fusion 6. BP reaction E with pDONR 221
18	lin-28 1st exon 3'(overlapping)	aggtgttggtga cgggagcctctcgaaggaag	
19	lin-28 2nd exon 5'(overlapping)	gagggctcccg tcaccaacacctcgatactttgg	
20	lin-28 100bp of 5' upstream	gttcagcaatgcttttaatta	
21	Primer for GFP fusionF	ggcgcgcctctagaggatc	
22	Primer for GFP fusion R(Overaping)	cggggatcctctagaggcgcgcc ttcatcagaggaattactattcttttc	
23	GFP R	ctatttgtatagttcatccatgcca	
24	attB2+lin-28::GFP gene R	ggggaccactttgtacaagaaagctgggtt ctatttgtatagttcatccatgcca	
25	attB2r+lin28_3UTR(5)	ggggcagctttcttgtacaaagtggga aatcatctagacactgagaata	lin-28 3'UTR:PCR ampliifed, follwed by BP reaction with pDONR P2R-P3
26	attB3 +lin-28_3UTR(3)	ggggcaactttgtataataaagttgt gccaacttgttgaggattgttaa	
27	ttTi5605 genotyping F	tgacattgtcgaaatgtcctc	ttTi5605: 1411bp transgene inserted: 7kb<
28	ttTi5605 genotyping R	gttatacagaagaccgttacg	
29	ttTi5605 genotyping 2F	tctggctctgcttcttcgtt	ttTi5605: 0bp transgene inserted: 1772bp
30	ttTi5605 genotyping 2R	caattcatcccggtttctgt	

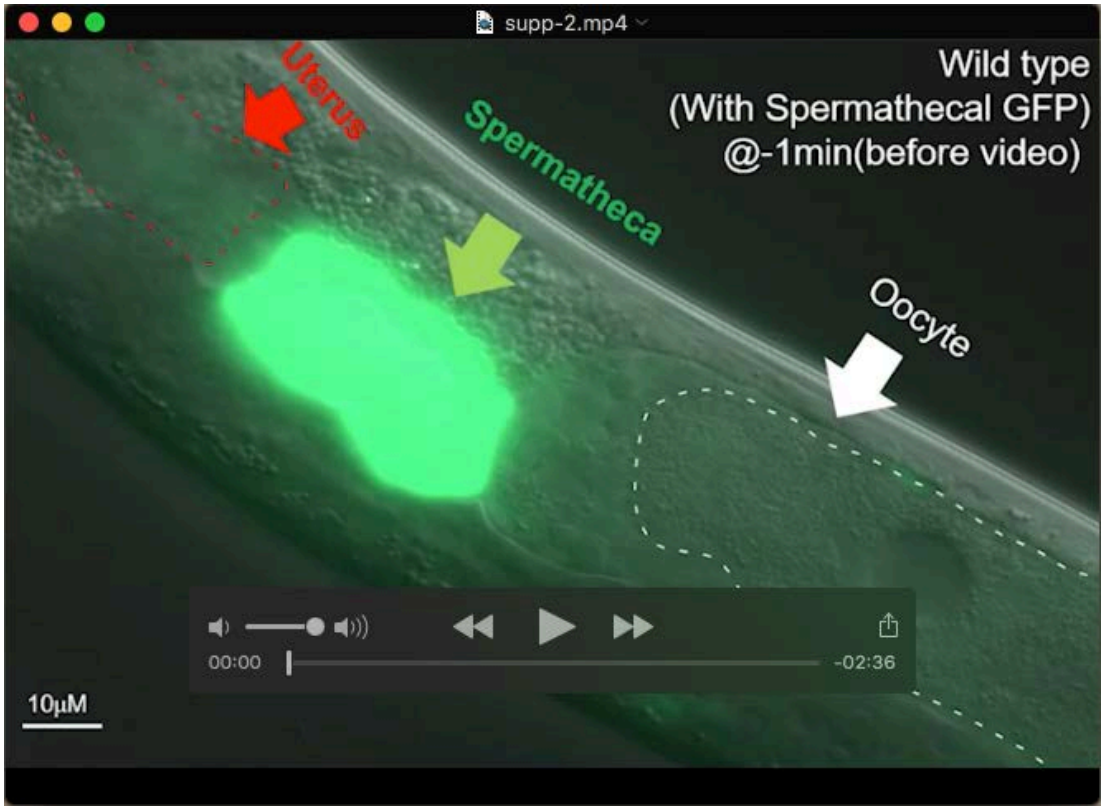

Movie 1. The first ovulation and spermathecal exit of a wild type animal

The first ovulation and spermathecal exit of a wild type animal (with *fkh-6p::GFP*, DZ325) was monitored using a time-lapse video taken for approximately 40 minutes. The first ovulation occurred around 20 minutes after the recording started, and spermathecal exit was completed approximately 15 minutes after the ovulation occurred. After the recording, a fertilized embryo was seen in the uterus.

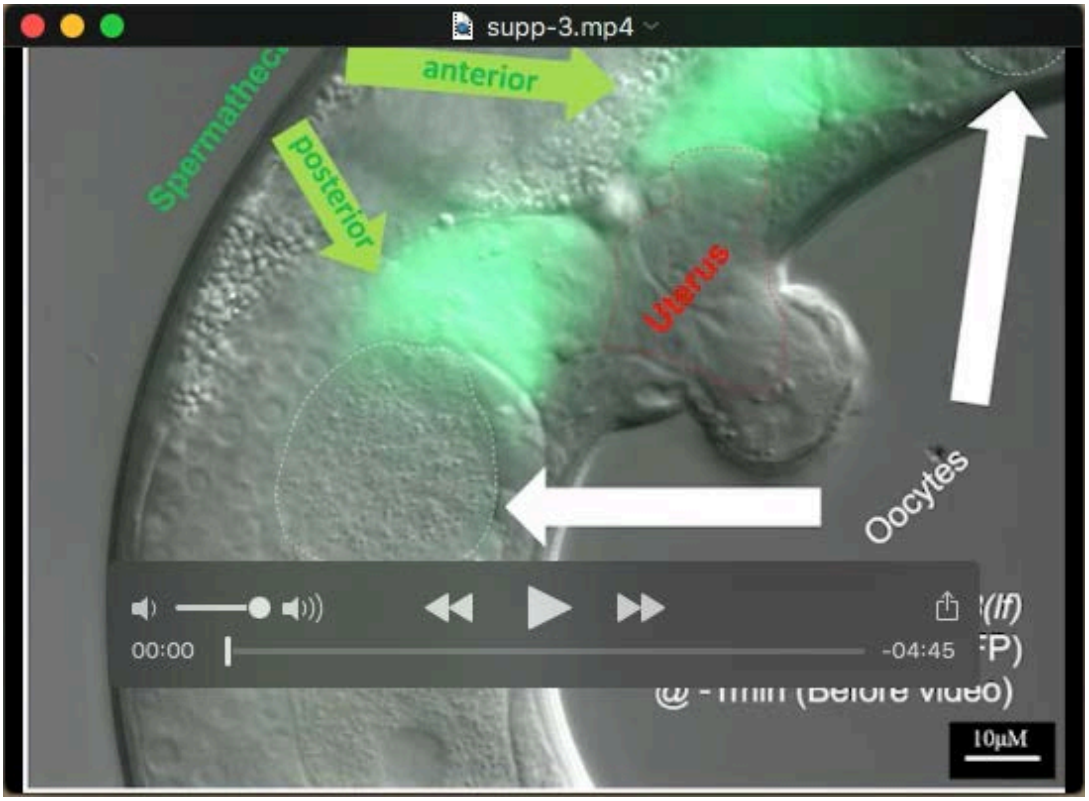

Movie 2. The first ovulation and defective spermathecal exit in each gonad arm of a *lin-28(lf)* mutant

The first ovulation and following process of a *lin-28(lf)* mutant (with *fkh-6p::GFP*, VT2930) was monitored using a time-lapse video. Two consecutive videos of one animal were taken for approximately 40 minutes each, with ~2 minutes of interval in between. The first ovulation in the posterior arm and the anterior arm occurred around 1~2 minutes, and 9~10 minutes after the recording started, respectively. However, the spermathecal exits of both ovulated embryos to the uterus were not completed approximately 82 minutes after the recording. As a result, parts of both embryos were seen in the spermathecal region labeled by *fkh-6:GFP*.